Journal of Molecular Structure 1072 (2014) 45–52

Contents lists available at ScienceDirect

Journal of Molecular Structure

journal homepage: www.elsevier.com/locate/molstruc

Determination of the geometry change of benzimidazole upon electronic excitation from a combined Franck–Condon/rotational constants fit

Benjamin Stuhlmann, Felix Gmerek, Daniel Krügler [1], Michael Schmitt *

Heinrich-Heine-Universität, Institut für Physikalische Chemie I, D-40225 Düsseldorf, Germany

HIGHLIGHTS

- Fluorescence excitation and single vibronic level fluorescence spectra of benzimidazole were recorded in a molecular beam.
- We determined the complete changes of the heavy atom structures in ground and lowest excited singlet states of benzimidazole.
- A combined Franck–Condon/rotational constants fit has been performed.
- Perturbations due to Herzberg–Teller coupling have been detected.

ARTICLE INFO

Article history:
Received 18 January 2014
Received in revised form 31 March 2014
Accepted 4 April 2014
Available online 6 May 2014

Keywords:
Franck–Condon analysis
Benzimidazole
Structure
Rotational constants
Herzberg–Teller

ABSTRACT

Single vibronic level fluorescence spectra of the electronic origin and of seven vibronic bands between 0,0 and 0,0 + 1265 cm^{-1} have been measured and analyzed by means of a combined Franck–Condon/rotational constants fit. The rotational constants in ground and lowest electronically excited singlet state of four different isotopologues have been taken from previous rotationally resolved measurements of Schmitt et al. (2006). The intensities of 182 vibronic emission bands and of 8 rotational constants have been used for a fit of the complete heavy atom geometry changes upon electronic excitation. Vibronic modes, about 1000 cm^{-1} above the electronic origin, show strong deviations from Franck–Condon behavior in emission. Herzberg–Teller coupling contributes to this effect. 1300 cm^{-1} above the origin, we observe the onset of intramolecular vibrational redistribution in the emission spectra.

Introduction

The combination of the information contained in the moments of inertia (or rotational constants), which are obtained from electronic rotationally resolved spectroscopy and of Franck–Condon factors from single vibronic level fluorescence (SVLF) spectroscopy, obtained by pumping various vibronic bands in the electronically excited states, provides reliable access to the structures of electronically excited states. A full substitution structure determination (referred to as r_s-structure) yielding Cartesian coordinates of each atom via Kraitchman analysis [1] of the moments of inertia of various isotopologues is in many cases unfeasible, since each atom in the molecule has to be replaced by one of its (stable) isotopologues. Information from multiple isotopic substitution cannot be integrated, except for some symmetric cases. A nonlinear fit of the structure in internal coordinates to the rotational constants on the other hand, has many advantages. Also multiply substituted isotopologues can be used in the analysis and relations between the parameters can easily be implemented, since the fit is performed in internal coordinates. Symmetry constraints like planarity in the case of benzimidazole or relations between the parameters can easily be introduced via the internal coordinates.

Electronically excited states can be distinguished via different molecular parameters. In practice, a combination of several of them is used for an unequivocal assignment of the excited states. By comparison to the results of *ab initio* calculations, the adiabatic excitation energy and the oscillator strength can give a preliminary answer. Other useful and often used state dependent molecular properties are the direction of the transition dipole moment and the absolute size and components of the permanent dipole moments of the excited states. The information, which is contained in the nuclear structure of the electronically excited state is much less used. In previous studies, we have shown, how the rotational constants of the excited state of indole, [2] of 7-azaindole, [3] its water clusters, [4] and of 5-cyanoindole [5] can be used as guidance for distinction of energetically close-lying excited states like the L_a- and L_b-states in indoles and related compounds.

* Corresponding author. Tel.: +49 0211 81 12100; fax: +49 211 81 15195.
E-mail address: mschmitt@uni-duesseldorf.de (M. Schmitt).
[1] Present address: Bremen.

http://dx.doi.org/10.1016/j.molstruc.2014.04.005
0022-2860/

Raman and polarized infrared spectra of partially oriented benzimidazole crystals were recorded by Suwaiyan et al. [6] Tomkinson gave a reassignment of the vibrational spectrum of benzimidazole up to 1300 cm^{-1} using inelastic neutron scattering spectroscopy. [7] Jalviste and Treshchalov [8] presented single vibronic level fluorescence (SVLF) spectroscopy and LIF spectroscopy of benzimidazole. Resonance enhanced multiphoton spectra of the monomer and several water clusters were studied by Jacoby et al. [9]. The microwave spectrum of benzimidazole in the vibrational ground state and two low-lying vibrational satellites have been measured by Velino et al. [10]. Rotational constants of benzimidazole in the excited states were obtained from a band contour analysis in the vapor phase by Cané et al. [11] and Berden et al. [12] Rotationally resolved electronic spectroscopy of four isotopologues of benzimidazole yielded the absolute orientation of the transition dipole moment and part of the changes of the structure upon electronic excitation. [13] Adiabatic ionization energies and the vibrational spectrum of the cationic ground state of benzimidazole were investigated with mass analyzed threshold ionization (MATI) by Lin et al. [14]. The HD exchange in benzimidazole was studied by Yang and Tzeng using MATI [15]. The lowest triplet state of benzimidazole (electronic origin at 26,536 cm^{-1}) was studied by Noda et al. [16] using electron paramagnetic resonance and optical detection of magnetic resonance in benzoic acid host crystals. Recently, an analysis of vibrational hot bands of benzimidazole has been given in our group [17].

Borin and Serrano-Andrés calculated the absorption spectrum of benzimidazole using the complete active space (CAS) SCF method and multiconfigurational second-order perturbation theory (CASPT2) [18]. The emission spectrum was calculated with the same theoretical methods by Serrano-Andrés and Borin [19].

In the present publication we present a Franck–Condon analysis of the fluorescence emission spectra through eight different vibronic bands of benzimidazole. Along with the data from rotationally resolved spectroscopy of four different benzimidazole isotopologues [13] a full determination of the geometry changes upon electronic excitation could be obtained.

Experimental and computational details

Experiment

The experimental setup for the dispersed fluorescence (DF) spectroscopy has been described in detail elsewhere [20,21]. In brief, benzimidazole was evaporated at 423 K and co-expanded through a pulsed nozzle with a 500 μm orifice (General Valve) into the vacuum chamber using Helium as carrier gas. The output of a Nd:YAG (SpectraPhysics INDI) pumped dye laser (Lambda-Physik, FL3002) was frequency doubled and crossed at right angles with the molecular beam. The resulting fluorescence was imaged on the entrance slit of a $f = 1$ m monochromator (Jobin Yvon, grating 2400 lines/mm blazed at 400 nm in first order). The dispersed fluorescence spectrum was recorded using a gated image intensified UV sensitive CCD camera (Flamestar II, LaVision). One image on the CCD chip spectrally covers approximately 600 cm^{-1}. Since the whole spectrum is taken on a shot-to-shot basis, the relative intensities in the DF spectra do not vary with the laser power. The relative intensities are afterwards normalized to the strongest band in the spectrum different from the resonance fluorescence band, which also contains the stray light and is therefore excluded from the FC analysis.

Ab initio calculations

Structure optimizations were performed employing Dunning's correlation consistent polarized valence triple zeta basis set (cc-pVTZ) from the TURBOMOLE library [22,23]. The equilibrium geometries of the electronic ground and the lowest excited singlet states were optimized using the approximate coupled cluster singles and doubles model (CC2) employing the resolution-of-the-identity approximation (RI). [24–26] Spin-component scaling (SCS) modifications to CC2 were taken into account [27]. The Hessians and harmonic vibrational frequencies for both electronic states, which are utilized in the FC fit have been obtained from numerical second derivatives using the NumForce script [28] implemented in the TURBOMOLE program suite [29].

Franck–Condon fit of the structural change

The change of a molecular geometry upon electronic excitation can be determined from the intensities of absorption or emission bands using the FC principle. According to the FC principle the relative intensity of a vibronic band depends on the overlap integral of the vibrational wave functions of both electronic states. The transition dipole moment for a transition between an initial electronic state $|m, v\rangle$ and a final electronic state $|n, w\rangle$ is defined as:

$$M_{vw} = \langle v|\mu_{mn}(Q)|w\rangle \tag{1}$$

with the electronic transition dipole moment $\mu_{mn}(Q)$:

$$\mu_{mn}(Q) = \langle \Psi_m|\mu|\Psi_n\rangle\mu = \sum_g e r_g \tag{2}$$

where r_g is the position vector of the gth electron. The dependence of the electronic transition dipole moment μ_{mn} on the nuclear coordinates can be approximated by expanding μ_{mn} in a Taylor series about the equilibrium position at Q_0. The series is truncated after the first term in the FC approximation.

The fit has been performed using the program FCFIT, which has been developed in our group and described in detail before [30,31]. The program computes the FC integrals of multidimensional, harmonic oscillators mainly based on the recursion formula given in the papers of Doktorov et al. [32,33] and fits the geometry (in linear combinations of selected normal modes) to the experimentally determined intensities. This is simultaneously done for all emission spectra, which are obtained via pumping through different S_1 vibronic modes.

The vibrational modes of the electronically excited state can be expressed in terms of the ground state modes using the following linear orthogonal transformation, first given by Duschinsky [34]:

$$Q' = SQ'' + d \tag{3}$$

where Q' and Q'' are the N-dimensional vectors of the normal modes of excited and ground state, respectively, S is a $N \times N$ rotation matrix (the Duschinsky matrix) and d is an N-dimensional vector which displaces the normal coordinates.

The fit of the geometry to the intensities in the vibronic spectra can greatly be improved if independent information for the geometry changes upon electronic excitation is available. This additional information is the change of the rotational constants upon electronic excitation, which can be obtained from rotationally resolved electronic spectroscopy. While geometry fits to the rotational constants (mostly of several isotopologues) are routinely performed using non-linear fits in internal coordinates, the combination of rotational constant changes and vibronic intensities allows for determination of many more geometry parameters.

Results

Ab initio calculations

The structure of benzimidazole in its ground and lowest excited singlet states has been determined from an optimization at the

second order coupled cluster (CC2) level of theory using the cc-pVTZ basis set. The atomic numbering, used throughout this publication is shown in Fig. 1. The Cartesian coordinates of the optimized structures of benzimidazole in the S_0, S_1, and S_2 states are given in the Online Supplementary Material. Benzimidazole is planar in both electronic states, as proven by the inertial defects in the electronic ground state [10] and in the lowest excited state [13] and belongs to the point group C_s. Of the 39 normal modes 12 are out-of-plane vibrations (A'') and 27 are in-plane (A').

The numbering of the 39 normal modes, their symmetries and their wavenumbers in the electronic ground and excited states are compiled in Table 1. The last column of this Table shows the largest elements of the Duschinsky matrix, which was calculated from the respective Hessians at the equilibrium positions and facilitates the assignments of ground states modes to excited state vibrations.

From the CC2/cc-pVTZ calculated excitations of the S_1 and the S_2 states, the character of the lowest electronically excited state has been determined to be L_b like (LUMO ← HOMO-1 and LUMO+1 ← HOMO) in the nomenclature of Platt[2], while the second excited singlet state is L_a like (LUMO ← HOMO).

Experimental results

The fluorescence excitation spectrum is similar to that, already shown in a variety of publications. It can be found in the Online Supplementary Material (Fig. S1) with the bands marked with an asterisk, that were used as excitation bands for obtaining the SVLF spectra. All observed intensities and the respective assignments of the transitions are compiled in Table S3 of the Online Supporting Material. We use the following convention for designation of vibrational levels and transitions: $(Q_{Mode\#})^n_m$ designates the vibronic transition with m quanta of $Q_{Mode\#}$ excited in the electronic ground state to n quanta of $Q_{Mode\#}$ excited in the electronically excited state. $(Q_{Mode\#})_m$ is the mth vibrational level of $Q_{Mode\#}$ in the ground state and $(Q_{Mode\#})^n$ the nth vibrational level of $Q_{Mode\#}$ in the electronically excited state.

The assignments of the vibronic bands in absorption and of the emission bands have been made on the basis of the results of the *ab initio* normal mode analysis presented in Table 1. In cases, where the assignments were not unequivocal, a FC simulation has been performed and the assignments checked, by the predicted intensities. In case of deviations, the assignments were iterated, until agreement with the wavenumbers from the *ab initio* calculations and the intensities from the FC simulations was obtained. All observed wavenumbers both in absorption and in emission, the transition intensities and the assignments are given in S3 and S4 of the Online Supplementary Material. Tentative assignments of vibrational hot bands have been given on the basis of combination differences using observed wavenumbers and their (harmonic) overtones.

Fig. 2 shows the SVLF spectrum of the electronic origin of benzimidazole at 36021.4 cm^{-1}, along with a FC simulation using the unaltered *ab initio* parameters (second trace) and a FC fit with the best fit parameters reported in S2 (third trace). In the FC simulation, the *ab initio* geometry of the ground and the excited state and the *ab initio* Hessians of both states are used without changes, while in the FC fit the geometry of the excited state is altered in order to minimize the squared deviations of the vibronic intensities and the changes of the rotational constants upon excitation. The general agreement between the experimental and the simulated and the fit spectrum is good. It is noteworthy, that already the simulation with the *ab initio* parameters reproduces the experimental spectrum closely. Deviations, like the too small intensities of Q_{20} and Q_{15} in the simulation, are corrected in the fit.

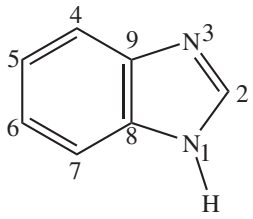

Fig. 1. Structure and atomic numbering of benzimidazole.

This means, that the geometry change upon electronic excitation is reasonably well described at the SCS-CC2/cc-pVTZ level of theory. The spectrum is dominated by in-plane modes, vibration Q_{24} being by far the most intense one. In the spectral region above 1500 cm^{-1} overtones and combination bands involving Q_{24} are found.

Fig. S2 of the Online Supporting Material shows the SVLF spectrum of the vibronic band at 0,0 + 303 cm^{-1}, along with a FC simulation using the *ab initio* parameters and a FC fit with the best fit parameters from S2. Two different assignments of 0,0 + 303 cm^{-1} seem possible. If the band is assigned to the fundamental of the Q_{37} out-of-plane motion (calculated at 296 cm^{-1}) the most intense emission band should be around 431 cm^{-1}, which is the respective mode according to the *ab initio* calculations for the electronic ground state. The strongest emission band is indeed found at 431 cm^{-1}, seemingly supporting this assignment. However, there should be no strong fundamental of an out-of-plane mode in a planar molecule with transition dipole moment in the plane of symmetry. Also, the emission spectrum is dominated by combination bands of in-plane vibrations with the excited, diagonal mode. This observation motivates a different assignment of the 0,0 + 303 cm^{-1} vibronic band. The first overtone of the lowest out-of-plane vibration Q_{39} can be deduced from the *ab initio* calculations assuming harmonicity for this mode to be 310 cm^{-1} (2×155 cm^{-1}, cf. Table 1). The respective vibration in the ground state would consequently be at 458 cm^{-1} (2×229 cm^{-1}), close enough to the experimental value to make this assignment the most probable one. Nevertheless, the agreement between the Franck–Condon simulation/fit with the experimental spectrum, shown in Fig. S2 of the Online Supporting Material, is considerably less than for all the in-plane modes. The reason for this obvious discrepancy can be found inspecting the elongation vectors of this mode. The out-of-plane vibration Q_{39} can best be described as a butterfly motion of the two rings. This motion is represented by a symmetric double minimum potential, and the harmonic approximation, which is the basis for the FC fit, completely fails.

Fig. S3 of the Online Supporting Material shows the SVLF spectrum of the vibronic band at 0,0 + 371 cm^{-1}, along with a FC simulation using the best fit parameters from S2. While the assignment of the excited state vibronic band to the fundamental of the Q_{35} out-of-plane mode (calculated at 360 cm^{-1}) seems possible, the mode with the largest Duschinsky coefficient in the ground state would be at 582 cm^{-1} in clear disagreement with an experimental value of 497 cm^{-1}. As in the case of the 303 cm^{-1} vibronic band, the assignment to an overtone of an out-of-plane vibration gives an unequivocal assignment: The overtone of Q_{35} in the excited state is calculated to be 366 cm^{-1}, close to the observed vibronic band. The diagonal transition leads to the ground state

[2] It should be pointed out that for molecules without at least C_{2v} symmetry the notations L_a and L_b are not based on symmetry arguments and in fact in the C_s case, as for benzimidazole, they belong to states with the same symmetry. These labels are merely a historic and convenient naming convention [36] to specify the lowest excited electronic singlet states. Nevertheless, Callis [37] has pointed out, that the transition densities in indole and benzimidazole can be correlated to those of the even membered perimeters, for which Platts original nomenclature has been developed.

Table 1
CC2/cc-pVTZ calculated and experimental wavenumbers of the 39 normal modes of the ground and first electronically excited states of benzimidazole along with the respective symmetry labels and those coefficients of the Duschinsky matrix, that are larger than 0.4.

Mode	S_0				S_1			Duschinsky
	Sym.	Calc.	Obs.[a]	Obs.[b]	Sym.	Calc.	Obs.	
$Q_1(S_0)$	A'	3657			A'	3637		$Q_1(S_1) = -1.00Q_1(S_0)$
$Q_2(S_0)$	A'	3267		3115	A'	3287		$Q_2(S_1) = -0.99Q_2(S_0)$
$Q_3(S_0)$	A'	3230		3079	A'	3249		$Q_3(S_1) = -0.88Q_3(S_0)$
$Q_4(S_0)$	A'	3221		3065	A'	3239		$Q_4(S_1) = -0.90Q_4(S_0)$
$Q_5(S_0)$	A'	3210		3040	A'	3224		$Q_5(S_1) = -0.77Q_5(S_0)$
$Q_6(S_0)$	A'	3200		3005	A'	3207		$Q_6(S_1) = -0.79Q_6(S_0)$
$Q_7(S_0)$	A'	1656			A'	1589	1565	$Q_8(S_1) = -0.90Q_7(S_0)$
$Q_8(S_0)$	A'	1615	1610	1620	A'	1515	1535	$Q_9(S_1) = -0.78Q_8(S_0)$
$Q_9(S_0)$	A'	1512			A'	1408	1425	$Q_{11}(S_1) = -0.55Q_9(S_0) + 0.53Q_{12}(S_0)$
$Q_{10}(S_0)$	A'	1500			A'	1432	1438	$Q_{10}(S_1) = -0.60Q_{10}(S_0) - 0.70Q_9(S_0)$
$Q_{11}(S_0)$	A'	1481		1478	A'	1382	1383	$Q_{12}(S_1) = +0.70Q_{11}(S_0) - 0.56Q_{12}(S_0)$
$Q_{12}(S_0)$	A'	1449		1412	A'	1603	1614	$Q_7(S_1) = +0.45Q_{12}(S_0) + 0.55Q_{11}(S_0)$
$Q_{13}(S_0)$	A'	1391	1363	1362	A'	1325	1323	$Q_{13}(S_1) = -0.80Q_{13}(S_0)$
$Q_{14}(S_0)$	A'	1323	1355	1353	A'	1256	1259	$Q_{15}(S_1) = +0.80Q_{14}(S_0)$
$Q_{15}(S_0)$	A'	1290	1270	1280	A'	1286	1297	$Q_{14}(S_1) = +0.89Q_{15}(S_0)$
$Q_{16}(S_0)$	A'	1269	1270	1251	A'	1219	1226	$Q_{16}(S_1) = -0.91Q_{16}(S_0)$
$Q_{17}(S_0)$	A'	1195	1188	1191	A'	1158		$Q_{17}(S_1) = -0.72Q_{17}(S_0) - 0.65Q_{18}(S_0)$
$Q_{18}(S_0)$	A'	1163	1157	1162	A'	1140	1136	$Q_{18}(S_1) = +0.73Q_{18}(S_0) + 0.17Q_{20}(S_0)$
$Q_{19}(S_0)$	A'	1122		1115	A'	1054	1043	$Q_{19}(S_1) = +0.89Q_{19}(S_0)$
$Q_{20}(S_0)$	A'	1093	1079		A'	893	887	$Q_{21}(S_1) = -0.60Q_{20}(S_0) + 0.64Q_{21}(S_0)$
$Q_{21}(S_0)$	A'	1021	1008	1007	A'	966	961	$Q_{20}(S_1) = -0.70Q_{21}(S_0) - 0.60Q_{20}(S_0)$
$Q_{22}(S_0)$	A'	928	928	935	A'	875	883	$Q_{22}(S_1) = -0.90Q_{22}(S_0)$
$Q_{23}(S_0)$	A'	881	891	890	A'	853	828	$Q_{23}(S_1) = +0.95Q_{23}(S_0)$
$Q_{24}(S_0)$	A'	780	777	770	A'	725	731	$Q_{24}(S_1) = +0.96Q_{24}(S_0)$
$Q_{25}(S_0)$	A'	617	622	619	A'	566	567	$Q_{25}(S_1) = +0.98Q_{25}(S_0)$
$Q_{26}(S_0)$	A'	542	545	544	A'	474	478	$Q_{26}(S_1) = -0.96Q_{26}(S_0)$
$Q_{27}(S_0)$	A'	407	409	422	A'	395	397	$Q_{27}(S_1) = -0.99Q_{27}(S_0)$
$Q_{28}(S_0)$	A''	953	959[c]		A''	760	766	$Q_{28}(S_1) = -0.92Q_{28}(S_0)$
$Q_{29}(S_0)$	A''	925		936	A''	656		$Q_{30}(S_1) = -0.61Q_{29}(S_0) - 0.49Q_{30}(S_0)$
$Q_{30}(S_0)$	A''	855	860[c]	851	A''	588		$Q_{32}(S_1) = +0.70Q_{30}(S_0) + 0.40Q_{34}(S_0)$
$Q_{31}(S_0)$	A''	847	841[c]	848	A''	626		$Q_{31}(S_1) = +0.52Q_{31}(S_0) - 0.61Q_{33}(S_0)$
$Q_{32}(S_0)$	A''	767	778[c]	752	A''	537	541	$Q_{33}(S_1) = -0.62Q_{32}(S_0) - 0.51Q_{34}(S_0)$
$Q_{33}(S_0)$	A''	750		748	A''	677	675	$Q_{29}(S_1) = -0.62Q_{33}(S_0) - 0.49Q_{29}(S_0)$
$Q_{34}(S_0)$	A''	648	653[c]	637	A''	521	532[c]	$Q_{34}(S_1) = -0.72Q_{34}(S_0) + 0.28Q_{33}(S_0)$
$Q_{35}(S_0)$	A''	582	593[c]	581	A''	360	358[c]	$Q_{36}(S_1) = -0.91Q_{35}(S_0)$
$Q_{36}(S_0)$	A''	458			A''	441		$Q_{35}(S_1) = -0.92Q_{36}(S_0)$
$Q_{37}(S_0)$	A''	431	428[c]	425	A''	296	295[c]	$Q_{37}(S_1) = -0.92Q_{37}(S_0)$
$Q_{38}(S_0)$	A''	255	249[c]	246	A''	183	186[c]	$Q_{38}(S_1) = -0.88Q_{38}(S_0)$
$Q_{39}(S_0)$	A''	229	216[c]		A''	155	152[c]	$Q_{39}(S_1) = -0.87Q_{39}(S_0)$

[a] Ground state vibrational wavenumbers from fluorescence emission spectra of this work.
[b] Out-of-plane (A'') vibrations from Raman crystal data [6], in plane (A') vibrations from IR (KBr mull) data [35].
[c] Out-of-plane vibrations from their overtones assuming perfectly harmonic behavior.

Table 2
Bond lengths of benzimidazole in picometer in the electronic ground and lowest excited singlet state from SCS-CC2 calculations utilizing the cc-pVTZ basis set and from the FC fit. The reference state for the geometry changes is the electronic ground state. Therefore, the geometry parameters for the ground state in FC fit have been taken from the SCS-CC2 calculations. For atomic numbering cf. Fig. 1.

State method	S_0		S_1		S_1–S_0	
	CC2	FCFit	CC2	FCFit	CC2	FCFit
N1C2	137.4	137.4	141.6	140.5	+4.2	+3.1
C2N3	131.8	131.8	132.4	132.7	+0.6	+0.9
N3C9	138.8	138.8	137.6	136.8	−1.2	−2.0
C9C4	139.9	139.9	141.0	142.0	+1.1	+2.1
C4C5	139.0	139.0	143.4	142.9	+4.4	+3.9
C5C6	140.9	140.9	143.0	142.3	+2.1	+1.4
C6C7	139.1	139.1	142.3	142.0	+3.2	+2.9
C7C8	139.6	139.6	141.6	141.8	+2.0	+2.2
C8C9	141.6	141.6	146.2	146.1	+4.6	+4.5
C8N1	138.0	138.0	136.0	136.0	−2.0	−2.0
N1H	100.7	100.7	100.8	100.7	+0.1	±0

vibrational level of 510 cm^{-1} (2 × 255 cm^{-1}), in good agreement with the experimental value of 497 cm^{-1}.

Since both vibronic bands at 303 and 371 cm^{-1} are due to motions, that cannot be described properly in the harmonic approximation, their emission intensities are excluded from the FC fit, and the respective spectra are only shown in the online supporting material.

The SVLF spectrum of the vibronic band at 0,0 + 397 cm^{-1} is shown in Fig. 3 along with a FC simulation using the geometries and Hessians from the CC2/cc-pVTZ *ab initio* calculations and with a FC fit, using the parameters for the geometry displacements given in S2. The excitation band has been assigned to the fundamental of the in-plane vibration Q_{27}. The dominating transition in emission is the diagonal $(Q_{27})_1^1$ band (apart from the resonance fluorescence $(Q_{27})_0^1$, which comes along with the stray light). All other bands, which have been assigned in the emission spectrum are combination bands of Q_{27} with other in-plane modes. In contrast to the SVLF spectra of the 0,0 + 303 cm^{-1} and the 0,0 + 371 cm^{-1} bands, the agreement between the experimental spectrum and the FC fit is nearly perfect.

The SVLF spectrum after excitation of the vibronic band at 0,0 + 566 cm^{-1} is given in Fig. 4, along with a FC simulation using the best fit parameters from S2. The excitation band in the

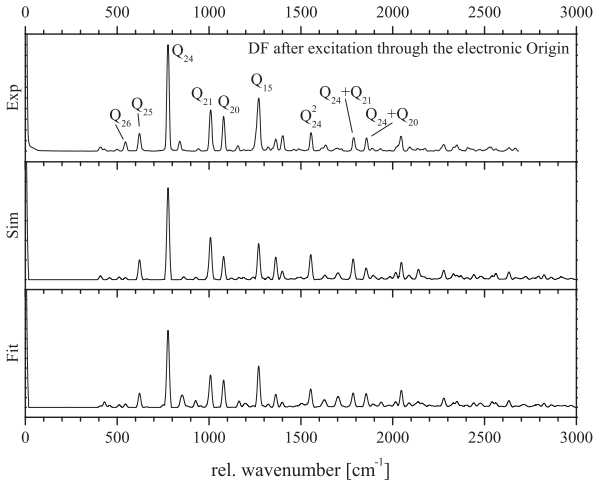

Fig. 2. SVLF spectrum of the electronic origin of benzimidazole along with a simulation using the *ab initio* parameters and a FC fit.

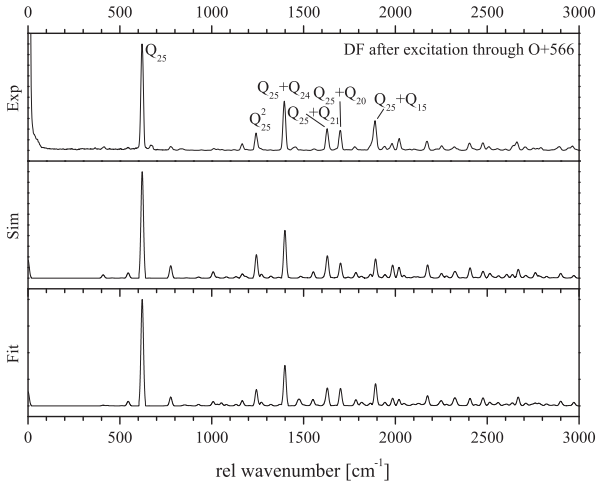

Fig. 4. (a) SVLF spectrum of the vibronic band at 566 cm^{-1}. (b) Simulation using the Geometries and Hessians from the CC2/cc-pVTZ *ab initio* calculations. (c) Best fit using the parameters for the geometry displacements given in S2.

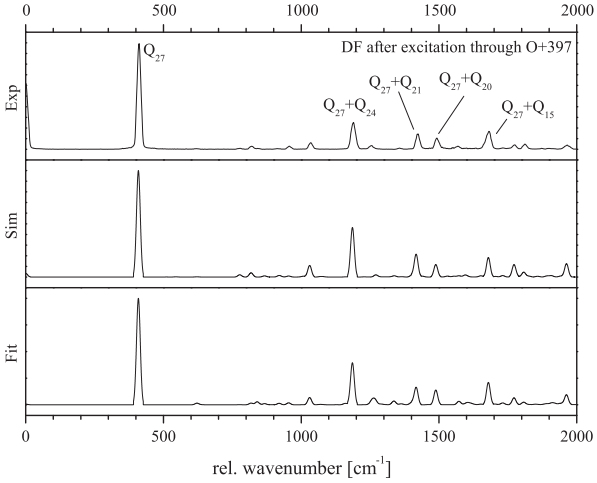

Fig. 3. (a) SVLF spectrum of the vibronic band at 397 cm^{-1}. (b) Simulation using the geometries and Hessians from the CC2/cc-pVTZ *ab initio* calculations. (c) Best fit using the parameters for the geometry displacements given in S2.

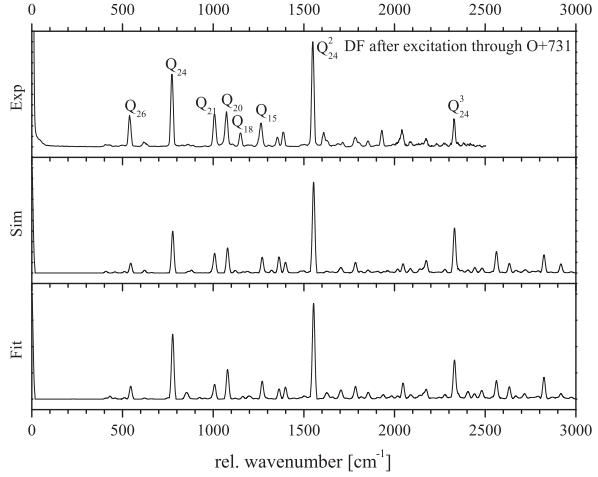

Fig. 5. (a) SVLF spectrum of the vibronic band at 731 cm^{-1}. (b) Simulation using the Geometries and Hessians from the CC2/cc-pVTZ *ab initio* calculations. (c) Best fit using the parameters for the geometry displacements given in S2.

absorption spectrum is assigned to the in-plane mode Q_{25}. The SVLF spectrum is dominated by the diagonal transition in Q_{25} and in overtones and combination bands containing this mode. Again a very close agreement between the experimental and the fit spectrum is found, as expected for an in-plane vibration (see Fig. 5).

The vibronic band at 0,0 + 731 cm^{-1} is assigned to the in-plane vibration Q_{24}. This mode already dominates the emission spectrum through the vibrationless origin. After excitation of this mode, the emission spectrum shows a long progression in Q_{24}, while no combination bands of Q_{24} with other in-plane vibrations show up. Good agreement between the fit and the experimental spectrum is found.

The vibronic band at 961 cm^{-1} in absorption is assigned to the in-plane mode Q_{20}. The emission spectrum through this band is shown in Fig. 6. Compared to the previous spectra the higher line density, the larger number of bands in the experimental spectrum which have no counterpart in the theoretical spectrum and the appearance of a non-resonant background is noticeable. Especially, the range 1200–1400 cm^{-1} around Q_{15} shows strong intensity deviations. The last trace (Fit*) gives the fit results from a FC fit of all other modes, with the modes Q_{20} and Q_{31} (see below) excluded from the fit.

Even larger deviations are observed for the emission spectrum through the vibronic band at 1265 cm^{-1}, shown in Fig. 7. This vibronic band is assigned to the overtone of the out-of-plane vibration Q_{31}. No satisfactory FC fit could be obtained for this emission spectrum, either. Although most bands are present in the fit, their intensities are much larger than in the experimental spectrum and there is a considerable background, which is much larger than in the spectrum of 0,0 + 961 cm^{-1}. The last trace (Fit*) gives the fit results from a FC fit of all other modes, with the modes Q_{31} and Q_{20} (see above) excluded from the fit.

Discussion

The intensities of the fluorescence emission bands after excitation of different vibronic bands have been fit using the program FCFIT, which was developed in our group [30,31,38]. Only emission band intensities, from excitation through in-plane vibrations have been taken into account, since the anharmonic nature of the out-of-plane vibrations, that describe the relative motions of the

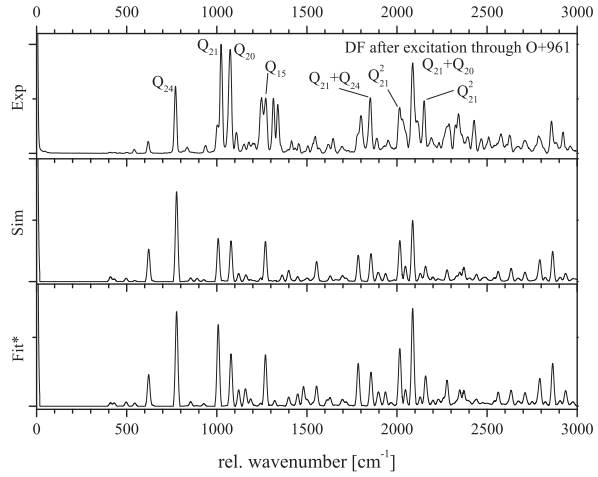

Fig. 6. (a) SVLF spectrum of the vibronic band at 961 cm^{-1}. (b) Simulation using the Geometries and Hessians from the CC2/cc-pVTZ *ab initio* calculations. (c) Best fit using the parameters for the geometry displacements given in S2.

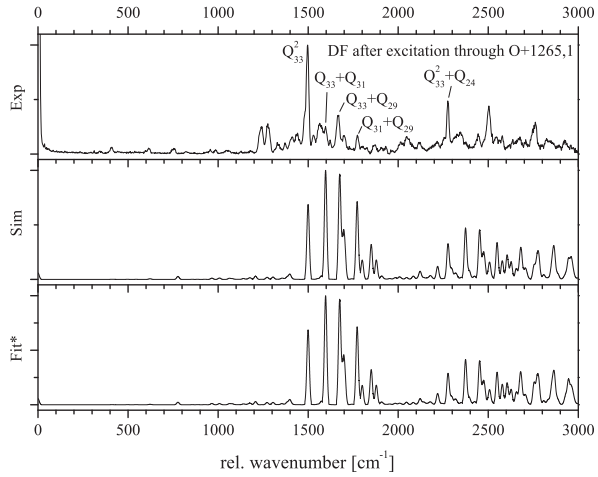

Fig. 7. (a) SVLF spectrum of the vibronic band at 1265 cm^{-1}. (b) Simulation using the Geometries and Hessians from the CC2/cc-pVTZ *ab initio* calculations. (c) Best fit using the parameters for the geometry displacements given in S2.

six- and the five-ring (butterfly and twist motion), prohibits the use of the FCFit model, which is based on the harmonic approximation. While in principle the use of out-of-plane vibrations is possible, as long as they are sufficiently harmonic, our model completely fails in the case of the energetically low lying butterfly and twist motions, which both are described by double minimum potentials in which tunneling through the barrier demands for linear combinations of the harmonic wave functions within each potential well.

Additionally, the changes of the rotational constants upon electronic excitation of four benzimidazole isotopologues, which have been taken from Ref. [13], have been used in the fit of the geometry changes. The ground state *ab initio* geometry was displaced along the 21 modes given in S2 of the online supporting material and the displacement varied until the combined χ^2 of the rotational constants and vibronic intensities were minimized. A total of 182 emission line intensities and of 12 rotational constants has been used to fit 21 displacement modes. Only 8 of the 12 rotational constants could be used in the fit independently, since the molecule is planar and in each isotopologue one of the three rotational constants can be expressed by the other two using the planarity relation $I_a - I_b - I_c = 0$. In principal $3N - 6$ geometry parameters are necessary to define the structure of a molecule in internal coordinates. However, in a planar molecule, the $3N - 3$ coordinates that define the dihedral angles are fixed and the complete geometry is determined by $2N - 3$ internal coordinates. Thus 27 independent geometry parameters are needed for a full description of the geometry or the geometry changes upon electronic excitation. The geometry changes of the four hydrogen atoms at the six-ring and of the hydrogen at C2 in the five-ring have been omitted from the fit, by excluding CH stretching vibrations from the basis for the molecular distortion. Since no safe assignments for the CH stretching region in the emission spectra could be given, their intensity fit would be too doubtful. Since we are mainly interested in the changes of the heavy atom structure, this is not a serious restriction.

Table 3 shows the good agreement between the experimental and fit values for the changes of the rotational constants of 1H2H, 1D2H, 1H2D, and 1D2D-benzimidazole (for numbering of the substitution position of the isotopologues refer to Fig. 1).

The geometry changes which have been calculated in the basis of the 21 normal mode displacements are expressed as bond length changes in Table 2 and the right half of Fig. 8 and are compared to the results of SCS-CC2 calculations. Good agreement is found between the FC and the *ab initio* calculated displacements. A more or less uniform expansion of the six-ring is accompanied by alternating expansions and contractions of the bond lengths in the five-ring (cf. Fig. 8).

The most FC active modes in the emission spectrum through the electronic origin are Q_{24}, Q_{23}, Q_{20}, and Q_{15}. Additionally to their strong intensities as fundamentals in the origin emission spectrum, they show up as overtones and/or combination bands through all of the emission spectra obtained via pumping different vibronic bands. Their distortion vectors, which are shown in Fig. 8 are indeed in good agreement with the geometry changes between the S_0 and S_1 states.

The emission intensities after pumping the two energetically highest vibronic bands at 961 and 1265 cm^{-1} have not been used in the FC fit of the geometry changes, due to large intensity deviations. They will be discussed in the following.

In the spectrum of the vibronic band at 0,0 + 961 cm^{-1} (the fundamental of mode Q_{20}), considerable deviations in the FC intensities between the experiment and the fit occur for some bands. While most of the intensities are well described, there are regions in the SVLF spectrum (mostly around Q_{15}) with quite a large number of additional bands in the experimental spectrum, displaying unexpectedly high intensities. They cannot be described properly within the Condon approximation made in the FC description of the spectra.

Perturbations due to Herzberg–Teller (HT) interaction to a higher lying electronic state are probably responsible for the appearance of the additional bands. Borin and Serrano-Andrés [19] calculated an adiabatic energy difference of 4000 cm^{-1} between the lower-lying L_b and the higher-lying L_a state at CASPT2 level and a difference in oscillator strength of a factor of two. Such a large energy difference to the perturbing state, along with a relatively small difference in oscillator strength would make HT interactions pretty small. Nevertheless, both states strongly mix, which has been shown by the orientations of the transition dipole moments [13], that are in disagreement with the predictions from the CASPT2 calculations. The three modes, that show the largest emission intensity differences between FC theory and experiment are Q_{16} at 1270 cm^{-1}, Q_{20} at 1079 cm^{-1} and Q_{21} at 1008 cm^{-1}. The left part of Fig. 9 gives the main contributions of the displacement vectors to the respective modes. On the right hand side, the main bond length differences between the optimized S_1 and S_2 structures from CASSCF calculations of Serrano-Andrés and Borin

Table 3
Experimentally determined changes of the rotational constants (in MHz) of the electronic origin band of four benzimidazole isotopologues from Ref. [13] along with the results of the FC fit. The numbering of the substitution positions refers to Fig. 1.

	1H2H		1D2H		1H2D		1D2D	
	Exp.	Fit	Exp.	Fit	Exp.	Fit	Exp.	Fit
ΔA/MHz	−155.72	−155.86	−149.98	−149.99	−156.27	−156.00	−150.26	−150.20
ΔB/MHz	−15.28	−15.12	−13.77	−13.78	−14.67	−14.56	−13.53	−13.33
ΔC/MHz	−21.40	−21.57	−20.47	−20.79	−20.65	−20.86	−19.85	−20.036

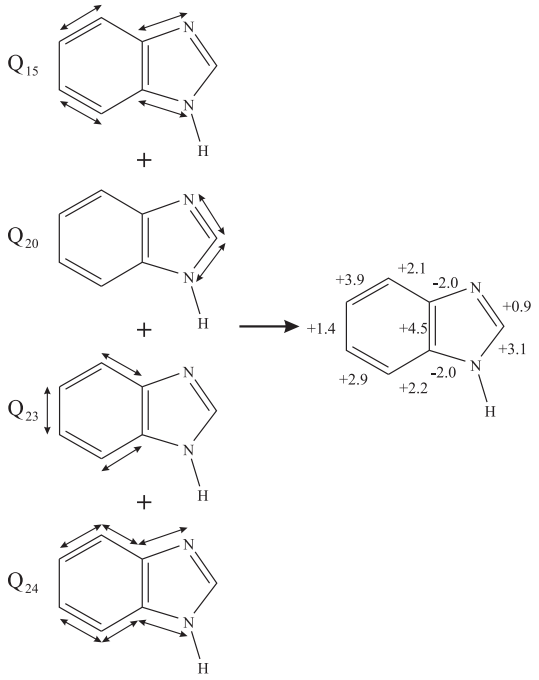

Fig. 8. Left: Main distortion vectors of the four most FC active vibrational modes Q_{24}, Q_{23}, Q_{20}, and Q_{15}. Right: Geometry differences in picometer between the optimized CC2/cc-pVTZ geometries of the S_0 and S_1 structures as given in Table 2.

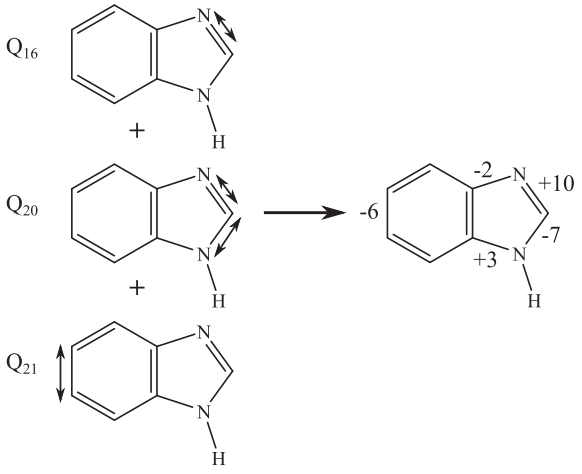

Fig. 9. Left: Main distortion vectors of the three vibrational modes Q_{16}, Q_{20} and Q_{21}, whose experimentally determined intensities are considerably larger, than expected from a pure FC fit. Right: Main geometry differences in picometer between the optimized S_1 and S_2 structures from CASSCF calculations in Ref. [19].

[19] are displayed. Comparison shows, that these three modes contribute strongly to the geometry differences between S_1 and S_2 state. Therefore, we expect them to be strong coupling modes for Herzberg–Teller perturbations, and their vibronic intensities will deviate from the pure FC intensities.

The experimental SVLF spectrum of the 0,0 + 1265 cm^{-1} band, assigned to the first overtone of the out-of-plane vibration Q_{31} finally shows very poor agreement with the FC fit. Many lines in the experimental spectrum are broadened, or even completely missing. We attribute this behavior to the onset of IVR in the excited state, coupling the bright zero-order state, which shows resonance fluorescence to the ground state to the bath of background states, from which sequence transitions to a multitude of ground state levels is possible, leading to an effective broadening of the emission spectrum. The onset of IVR at about 1300 cm^{-1} is in agreement with the finding for similar molecules like indole [39].

Conclusions

Using the combined information from SVLF spectra and rotational constants we were able to fit the complete structural changes of benzimidazole upon electronic excitation to the lowest excited singlet state. Since the basis for the geometry changes is of equal size as the $2N-3$ coordinates, that are needed for a full description of the geometry of a planar molecule, and thus no further model approximations have to be made, the agreement between *ab initio* calculated and FC fit bond length displacement is good. Even, if only a relatively small number of inertial data from different isotopologues is at hand, the addition of a sufficient number of intensity data from various SVLF spectra can add sufficient information for a reliable determination of the structural changes upon electronic excitation.

Acknowledgments

The authors like to thank the Universitätsrechenzentrum Köln for the granted computing time on Cheops. The financial support of the Deutsche Forschungsgemeinschaft (SCHM 1043/12) is gratefully acknowledged.

Supplementary material

Supplementary data associated with this article can be found, in the online version, at http://dx.doi.org/10.1016/j.molstruc.2014.04.005.

References

[1] J. Kraitchman, Am. J. Phys. 21 (1953) 17.
[2] J. Küpper, D.W. Pratt, W.L. Meerts, C. Brand, J. Tatchen, M. Schmitt, Phys. Chem. Chem. Phys. 12 (2010) 4980–4988.
[3] M. Schmitt, C. Ratzer, K. Kleinermanns, W.L. Meerts, Mol. Phys. 102 (2004) 1605–1614.
[4] Y. Svartsov, M. Schmitt, J. Chem. Phys. 128 (2008). 214310(1–9).
[5] O. Oeltermann, C. Brand, B. Engels, J. Tatchen, M. Schmitt, Phys. Chem. Chem. Phys. 14 (2012) 10266–10270.
[6] A. Suwaiyan, R. Zwarich, N. Baik, J. Raman Spectrosc. 21 (1990) 243–249.
[7] J. Tomkinson, J. Phys. Chem. A 112 (2010) 6115–6119.
[8] E. Jalviste, A. Treshchalov, Chem. Phys. 172 (1993) 325.

[9] C. Jacoby, W. Roth, M. Schmitt, Appl. Phys. B 71 (2000) 643.
[10] B. Velino, A. Trombetti, E. Cané, J. Mol. Spectrosc. 152 (1992) 434–440.
[11] E. Cané, A. Trombetti, B. Velino, W. Caminati, J. Mol. Spectrosc. 150 (1991) 222.
[12] G. Berden, W.L. Meerts, E. Jalviste, J. Chem. Phys. 103 (1995) 9596–9606.
[13] M. Schmitt, D. Krügler, M. Böhm, C. Ratzer, V. Bednarska, I. Kalkman, W.L. Meerts, Phys. Chem. Chem. Phys. 8 (2006) 228–235.
[14] J.L. Lin, Y.C. Li, W.B. Tzeng, Chem. Phys. 334 (2004) 189–195.
[15] S.C. Yang, W.B. Tzeng, Chem. Phys. Lett. 501 (2010) 6–10.
[16] M. Noda, S. Nagaoka, N. Hirota, Bull. Chem. Soc. Jpn. 57 (1984) 2376–2386.
[17] C. Brand, J. Rolf, M. Wilke, M. Schmitt, J. Phys. Chem. A 117 (2014) 12812–12820.
[18] A.C. Borin, L. Serrano-Andrés, Chem. Phys. 262 (2000) 253–265.
[19] L. Serrano-Andrés, A.C. Borin, Chem. Phys. 262 (2000) 267–283.
[20] M. Schmitt, U. Henrichs, H. Müller, K. Kleinermanns, J. Chem. Phys. 103 (1995) 9918–9928.
[21] W. Roth, C. Jacoby, A. Westphal, M. Schmitt, J. Phys. Chem. A 102 (1998) 3048–3059.
[22] R. Ahlrichs, M. Bär, M. Häser, H. Horn, C. Kölmel, Chem. Phys. Lett. 162 (1989) 165–169.
[23] J.T.H. Dunning, J. Chem. Phys. 90 (1989) 1007–1023.
[24] C. Hättig, F. Weigend, J. Chem. Phys. 113 (2000) 5154–5161.
[25] C. Hättig, A. Köhn, J. Chem. Phys. 117 (2002) 6939–6951.
[26] C. Hättig, J. Chem. Phys. 118 (2002) 7751–7761.
[27] A. Hellweg, S. Grün, C. Hättig, Phys. Chem. Chem. Phys. 10 (2008) 1159–1169.
[28] P. Deglmann, F. Furche, R. Ahlrichs, Chem. Phys. Lett. 362 (2002) 511–518.
[29] TURBOMOLE V6.3 2012, a development of University of Karlsruhe and Forschungszentrum Karlsruhe GmbH, 1989–2007, TURBOMOLE GmbH, since 2007. <http://www.turbomole.com>.
[30] D. Spangenberg, P. Imhof, K. Kleinermanns, Phys. Chem. Chem. Phys. 5 (2003) 2505–2514.
[31] R. Brause, M. Schmitt, D. Spangenberg, K. Kleinermanns, Mol. Phys. 102 (2004) 1615–1623.
[32] E.V. Doktorov, I.A. Malkin, V.I. Man'ko, J. Mol. Spectrosc. 56 (1975) 1–20.
[33] E.V. Doktorov, I.A. Malkin, V.I. Man'ko, J. Mol. Spectrosc. 64 (1977) 302–326.
[34] F. Duschinsky, Acta Physicochim. U.R.S.S. 7 (1937) 551–577.
[35] M. Cordes, J.L. Walter, Spectrochim. Acta A 24 (1968) 1421–1435.
[36] J.R. Platt, J. Chem. Phys. 17 (1949) 484–495.
[37] P.R. Callis, Int. J. Quantum Chem. 18 (1984) 579.
[38] M. Böhm, J. Tatchen, D. Krügler, K. Kleinermanns, M.G.D. Nix, T.A. LeGreve, T.S. Zwier, M. Schmitt, J. Phys. Chem. A 113 (2009) 2456–2466.
[39] D.A. Dolson, K.W. Holtzclaw, S.H. Lee, S. Munchak, C.S. Parmenter, B.M. Stone, Laser Chem. 2 (1983) 271–283.